Open access • Journal Article • DOI:10.1039/C9RE00245F

Kinetic evaluation of chitosan-derived catalysts for the aldol reaction in water

Anton De Vylder, Jeroen Lauwaert, Jeriffa De Clercq, Pascal Van Der Voort ...+2 more authors

Institutions: Ghent University

Published on: 22 Oct 2019 - Reaction Chemistry and Engineering (The Royal Society of Chemistry)

Topics: Imine, Chitosan, Aldol reaction, Catalysis and Aqueous solution

Kinetic Evaluation of Chitosan Derived Catalysts for the Aldol Reaction in Water

Received 00th January 20xx,
Accepted 00th January 20xx

DOI: 10.1039/x0xx00000x

Anton De Vylder[a], Jeroen Lauwaert[b], Jeriffa De Clercq[b], Pascal Van Der Voort[c], Christian V. Stevens[d], Joris W. Thybaut[a,*]

The site time yield (STY) and stability of the primary amine sites in low molecular weight chitosan has been quantified for the aldol reaction of acetone with 4-nitrobenzaldehyde in a mixture of water and acetone as solvent. Crude chitosan with varying degrees of deacetylation (DDA), as well as chitosan in hydrogel and aerogel form was used. Apart from the main reaction, accumulation of an imine formed from 4-nitrobenzaldehyde occurred in the early stages of the reaction. This imine acted as an inhibitor of the primary amine sites and was formed until an equilibrium was reached, after which the catalytic activity remained constant. Chitosan with a DDA amounting to 70.4% exhibited a STY of 2.18 ± 0.05 10^{-5} $mol_{product}$ mol_{amine}^{-1} s^{-1}. This STY increased with a decreasing DDA, as a direct result of an increase in amine pKa. No differences in activity were observed between the crude, hydrogel, or aerogel forms of chitosan with the same DDA. Recycling in a second batch experiment allowed reproducing the same performance as in the first experiment. Under continuous-flow conditions, the activity of chitosan was found to stabilize as a function of the time on stream, after the imine formation has equilibrated. Even though the catalytic activity of these chitosan catalysts was found to be lower than the current state-of-the-art catalysts for the aldol reaction, their stability in an aqueous environment opens up new perspectives for future catalyst development.

Introduction

Chitin is one of the most abundant biopolymers in nature, obtained from crab- and shrimp shell waste, and is composed almost entirely of β-(1-4)-N-acetyl-D-glucosamine units[1]. Partial deacetylation of chitin yields a copolymer consisting of both β-(1-4)-N-acetyl-D-glucosamine and D-glucosamine units, denoted as chitosan, see Figure 1. The primary amines that are made accessible by deacetylation have proven their use for a variety of applications, e.g., for their chelating ability in removal of heavy metal ions from aqueous streams[2, 3], their biocompatibility for nanofibrous pH sensors[4], and their antibacterial and antifungal properties[5, 6]. Moreover, they have also served as catalytic sites for various organic reactions, such as the aldol[7-11], nitroaldol[10] and knoevenagel reaction[7, 10], or for anchoring novel catalytic sites[12-14].

This work focuses on the aldol reaction, which is an important carbon-carbon coupling reaction that has applications in the pharmaceutical industry[15], fine-chemical synthesis[16, 17], and in the production of biomass-derived hydrocarbon fuels[18, 19]. At the commercial scale, these processes are typically performed in the presence of an organic solvent, while more sustainable solutions with either water as solvent or solvent-free, i.e. using the reactant aldehyde or ketone as a solvent, are being pursued[20, 21].

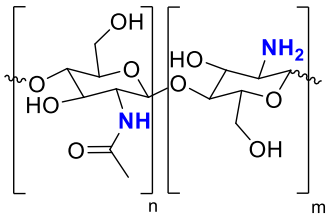

Figure 1: Structure of chitosan, consisting of n β-(1-4)-N-acetyl-D-glucosamine units and m D-glucosamine units.

Another research focus is the development of heterogeneous catalysts that can replace the frequently employed homogeneous catalysts. Related advantages are a reduced energy cost for separating the catalyst from the product stream, a longer catalyst lifetime, and reduced equipment corrosion[22, 23]. Examples of heterogeneous candidate catalysts for the aldol reaction are solid acid type catalysts, such as zeolites[24, 25], solid bases such as hydrotalcite based materials[26, 27], or amine functionalized mesoporous silica catalyst[28-33]. Both primary and secondary amines on silica catalyze the aldol reaction through an enamine intermediate[32]. However, in organic solvents, primary amines form stable imines that inhibit the catalytic activity[34]. Secondary amines cannot form these imines and are therefore typically found to exhibit a higher catalytic activity, provided that the access to the amine site is not sterically hindered[35-37]. Although, it does appear that this activity order can be reversed when using water as a co-solvent with acetone due to water shifting the equilibrium away from the inhibiting imine[34]. For these amine functionalized mesoporous silica catalysts, it has been observed that the residual silanol groups on the surface of the support act cooperatively with the grafted amines, thereby increasing the turnover frequency[31, 32]. More recent work demonstrated that the reusability of these grafted amine sites could be significantly enhanced if a few percentages of water are added to the aldol reaction mixture[33]. However, larger amounts of water lead to hydrolysis of the silica support and subsequent loss of the active sites[33, 38]. Hence,

[a] Laboratory for Chemical Technology (LCT), Department of Materials, Textiles, and Chemical Engineering, Ghent University, Technologiepark 125, 9052 Ghent, Belgium
[b] Industrial Catalysis and Adsorption Technology (INCAT), Department of Materials, Textiles, and Chemical Engineering, Ghent University, Valentin Vaerwyckweg 1, 9000 Ghent, Belgium.
[c] Center for Ordered Materials, Organometallics and Catalysis (COMOC), Department of Chemistry, Ghent University, Krijgslaan 281-S3, 9000 Ghent, Belgium
[d] SynBioC Research Group, Department of Green Chemistry and Technology, Ghent University, Coupure Links 653, 9000 Ghent, Belgium
* Corresponding author: Joris Thybaut (Joris.Thybaut@UGent.be)
Electronic Supplementary Information (ESI) available: See DOI: 10.1039/x0xx00000x

improvement of the support stability in an aqueous environment is an important next step in the development of a stable heterogeneous amine catalyst for the aldol reaction. Amines immobilized on organic polymers, as is the case in chitosan, thus present themselves as ideal candidate catalysts. The mechanism of the often investigated model aldol reaction of acetone with 4-nitrobenzaldehyde, catalyzed by primary amines such as found on chitosan, has been elucidated previously[32, 39] and is shown in Figure 2 by the black arrows. It starts with the addition of acetone to the primary amine (**1**) and subsequent formation of a carbinolamine intermediate (**2**). This carbinolamine then dehydrates towards an imine intermediate (**3**), which is in equilibrium with its enamine form (**4**) via an intramolecular proton transfer. The enamine is sufficiently nucleophilic to bind an incoming 4-nitrobenzaldehyde species and form a new carbon-carbon bond, resulting in the formation of an imine intermediate (**5**). Hydration of this imine intermediate (**5**) yields a carbinolamine (**6**) that detaches from the active site as the aldol product (**7**), thereby restoring the catalytic site (**1**). A possible side-reaction is the formation of an imine species (**8**) originating from 4-nitrobenzaldehyde[36], which is represented by the grey arrows in Figure 2.

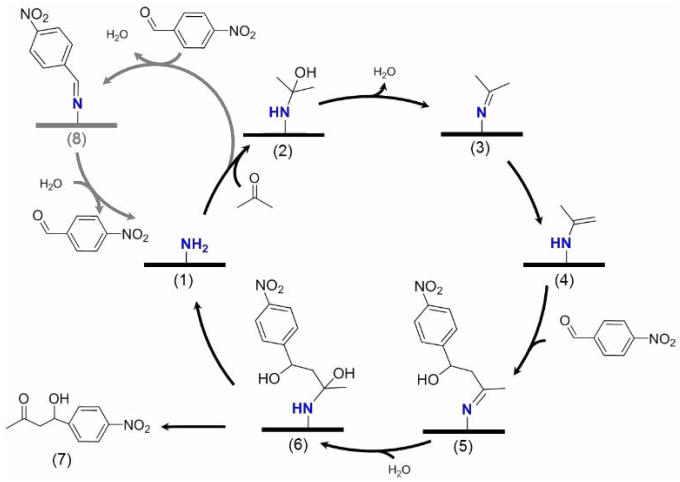

Figure 2: Reaction mechanism for the aldol reaction of acetone with 4-nitrobenzaldehyde on the primary amines of chitosan catalysts, based on reference 32.

In recent years, it has been shown that chitosan in its crude, hydrogel, or aerogel form is able to catalyze the aldol reaction[7-11]. Kantam et al.[7] reported complete conversion in the aldol reaction of 4-nitrobenzaldehyde with acetone with chitosan hydrogels, using dimethyl sulfoxide (DMSO) and acetone as solvent. No conversion was observed when chitosan powder was employed under the same reaction conditions. Quignard et al.[8, 9] were the first to recognize the need of water as co-solvent to obtain meaningful conversion levels in the aldol reaction catalyzed by crude chitosan and chitosan aerogels. They concluded that comparable conversion levels can be reached with both the hydrogel, aerogel, and crude form of chitosan[8]. Diaz et al.[10] were unable to reproduce these conversion levels and highlighted the importance of a meticulous washing procedure of the hydrogels to avoid residual hydroxide ions catalyzing the aldol reaction. Kayser et al.[11] reported that chitosan aerogels are catalytically active in the aldol reaction of furfural and acetone, provided that water is present, and obtained full conversion in 4 hours. Hence, these research groups have already shown that chitosan can be used to obtain a high total conversion in the aldol reaction, both in its crude, hydrogel and aerogel form. However, to the best of our knowledge, no quantification of the reaction rate or reusability ratio has yet been performed for chitosan as heterogeneous catalyst in the aldol reaction.

Meanwhile, it has become clear that the beneficial effect of water in the chitosan catalyzed aldol reaction can be attributed to the molecular structure of chitosan[40]. Because of the abundant presence of amino and hydroxyl groups in the polymer chain of both chitin and chitosan, a hydrogen-bond network is formed between these moieties in an organic solvent, leading to partial crystallization and poor accessibility of the amine sites on the polymer[13]. Water breaks this intramolecular hydrogen-bond network, and allows both chitin[41] and chitosan to swell[13, 42]. This improved accessibility leads to a higher catalytic activity being observed when crude chitosan is used in the aqueous aldol reaction[8] or when hydrogels are used[7]. Therefore, in combination with previous work performed on the beneficial effect of water on the amine site stability in the aldol reaction[33, 34, 36], a mixture of water and acetone as excess reagent is employed as solvent in this work. It should, however, be noted that the requirement of water for obtaining a stable and active catalyst limits the scope of this work to water soluble aldehyde and ketone reagents.

The catalytic activity of chitosan, which is an important feature to evaluate its potential industrial viability, is evaluated in this work for a first and second run in a batch reactor[43]. The activity and reusability of the primary amine sites in chitosan for the aldol reaction is then compared to the silica-based heterogeneous amine catalysts[35]. Finally, the long-term stability of chitosan as catalyst in the aldol reaction is evaluated in a continuous-flow reactor setup.

Procedures

Catalyst Synthesis

Crude low-molecular weight chitosan (Sigma Aldrich, low molecular weight = 50000 - 190000 Da) and crude chitin (Sigma Aldrich, practical grade, coarse flakes, from shrimp shells) were used as received without further purification. The hydrogel form was synthesized by first dissolving 5 g of the low molecular weight chitosan powder in 200 mL of an acetic-acid solution (50 mM in water) and stirring for 24 hours. The resulting solution was then added dropwise into a 4 M NaOH-solution in water with a syringe equipped with a needle (ø 0,08 mm) leading to reprecipitated hydrogels with a diameter of ± 2 mm. Previous research has shown that this procedure results in chitosan hydrogels with a crystallinity that is comparable to hydrated chitosan[44]. After 10 hours of hardening, the hydrogels were filtered on a Buchner filter and washed with deionized water. For the complete removal of the entrapped NaOH, the

hydrogels were placed in 1 L deionized water and gently stirred at 60 rpm for 4 hours before being filtered off. This washing step was repeated until the pH-value of the washing water was neutral and then, to ensure no NaOH remained entrapped in the pores[10], this was repeated three more times. To determine the water content in the hydrogels, part of the hydrogel beads were dried overnight at 120 °C and the correspondingly obtained dry mass was then compared to the wet mass. Aerogels were prepared by freezing the hydrogels to -80 °C and then placing them for 24 hours in a freeze-dryer (Alpha 1-2 LDplus), operating at 0.12 mbar.

Chitosan with different degrees-of-deacetylation was synthesized according to literature[45]. The coarse chitin flakes were first pulverized, after which they were immersed in a 12.5 M NaOH-solution, employing a volumetric solid-to-solvent ratio of 1:5, at 100 °C. The reaction times were varied between 2 and 24 hours to obtain a range of deacetylation degrees. To completely remove all residual NaOH, the same washing procedure as described above for the hydrogels was applied. Afterwards, the chitosan was dried at 70 °C for 24 hours.

Catalyst Characterization

Elemental CHN analysis was used to quantify the degree-of-deacetylation (DDA) of the chitosan samples, as it is one of the few accurate methods that are applicable in the full deacetylation range[46-48]. These experiments were performed on a Thermo Flash 2000 elemental analyzer. The DDA was calculated from the carbon/nitrogen ratio (C/N), which varies from 5.145 in completely deacetylated chitosan ($C_6H_{11}O_4N$) to 6.861 in fully acetylated chitin ($C_8H_{13}O_5N$), according to (eq. 1).

$$\mathrm{DDA} = 1 - \left(\frac{{}^{\mathrm{C}}/_{N} - 5.145}{6.861 - 5.145}\right) \qquad \text{(eq. 1)}$$

Infrared spectroscopy on crude chitosan and spent chitosan was performed on a Tensor II (Bruker). Background correction was performed with KBr (Sigma-Aldrich, FR-IR grade, >99%). The sample was measured between 600 cm^{-1} and 4000 cm^{-1}. Before analysis, the spent chitosan was washed and filtered twice using 1 L of double deionized water, to remove products and unreacted reagents.

Repeat CHN characterizations have indicated that the experimental error on the DDA, calculated as the 95% confidence interval, was 3.5%.

Performance Evaluation

The aqueous aldol reaction of acetone (99.6%, Acros) with 4 nitrobenzaldehyde (99%, Acros), yielding 4-hydroxy-4-(4-nitrophenyl)butan-2-one as aldol product and 4-(4-nitrophenyl)-3-buten-2-one as enone product, was selected as the model reaction, see Scheme 1. Two batch reactors have been used to measure the kinetics of this reaction, i.e., a Parr reactor and a glass flask. Consecutive batch experiments with recycled chitosan were performed for the hydrogel and aerogel type. No recycle experiments were performed with crude chitosan as a catalyst, because of difficulties in filtering the fine powder. Instead, the catalytic stability of crude chitosan was evaluated in a packed-bed continuous-flow reactor.

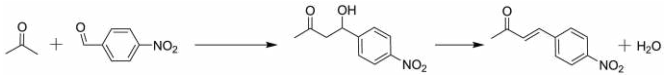

Scheme 1: Aldol reaction of acetone and 4-nitrobenzaldehyde towards the primary aldol product 4-hydroxy-4-(4-nitrophenyl)butan-2-one, and subsequent dehydration to the secondary enone product 4-(4-nitrophenyl)-3-buten-2-one.

A limited, non-heterogeneously catalyzed conversion of 4-nitrobenzaldehyde towards the aldol reaction products occurred when using water as solvent, as displayed for the batch reactor in Figure 1S in the Supplementary Information. This has also been observed by other research groups[49, 50]. In this work, the amount of catalyst is determined such that the obtained yields are always significantly higher than this background reaction in water.

Batch Reactor. The detailed procedure for operating the Parr® 4560 mini reactor has been reported previously[33] and is briefly summarized here. The reactor was first loaded with 0.26 g crude chitosan, 55.0 g water as solvent (deionized, Milli-Q®), and 0.25 g methyl 4-nitrobenzoate (> 99%, Sigma-Aldrich) as internal standard. This mixture was then heated to 55 °C, under constant stirring at 400 rpm. Acetone (45 g) was separately heated to 55 °C, and was then used to dissolve 0.45 g 4-nitrobenzaldehyde immediately before injecting in the reactor. The temperature in the reactor was maintained at 55 °C using a PID-controller (CAL 9500P), with a thermocouple inside the reactor vessel. This PID controller steered both an electrical heating jacket as well as a cooling unit for an adequate temperature control. The time of injection of the acetone/4-nitrobenzaldehyde mixture in the reactor was taken as the start of the reaction (t = 0). The reaction was monitored for 4 hours by taking a sample (0.3 mL) of the reaction mixture every 30 minutes.

To avoid breaking the hydrogel beads by vigorous mechanical stirring, smaller scale experiments in glassware were also performed for the chitosan hydrogel beads. For these experiments, 22.5 g acetone, 27.5 g deionized water, 0.23 g 4-nitrobenzaldehyde, 0.11 g methyl 4-nitrobenzoate were added to a 250 mL flask and stirred at 250 rpm in an oil bath at 55 °C. The temperature in the oil bath is controlled by a thermocouple (ETS-D5 IKA RCT) and a water cooled reflux condenser is used to seal the flask. The mixture was allowed to reach the isothermal reaction temperature during 30 minutes, after which the hydrogel catalyst (an equivalent of 0.05 g crude chitosan) is added. This time is taken as t = 0. Samples (0.3 mL) were drawn from the reaction mixture every hour for 4 hours. For each experiment, the total decrease of reaction volume due to sampling was less than 5% whereby the effect of sampling on the kinetic data is considered to be negligible. Repeat experiments have been performed to assess the experimental error, calculated as the 95% confidence interval.

To recycle the catalyst for a second run, the hydrogel and aerogel catalyst beads were filtered from the reactor with a Buchner filter. The reactor was briefly rinsed with deionized water to ensure all the beads were removed. The filtered beads were then stored in a glass flask and recycled for the second batch experiment within 24 hours.

Continuous-flow reactor. Stability tests were performed in an in-house developed liquid-phase packed-bed tubular reactor, loaded with 1 g of crude chitosan. The operating procedure has already been reported previously[33], and is briefly summarized here. The feed mixture was fed at the top of the reactor with a HPLC pump (Eldex Laboratories model 2SMP) at a rate of 1.5 ml min^{-1}. The feed composition was equivalent to the batch reactor feed composition, consisting of 0.45 wt% 4-nitrobenzaldehyde, 44.6 wt% acetone, 54.5 wt% deionized water and 0.25 wt% methyl 4-nitrobenzoate as internal standard. The space time, determined as $\frac{W_{cat}}{F^0_{feed}}$, was $1510\ kg_{cat}\ s\ mol^{-1}{}_{4NB}$. The non-heterogeneously catalyzed total product yield at these conditions was determined at 1.69 % and is subtracted from the results. The reactor itself is electrically heated, with its temperature being controlled at 55 °C by an outer thermocouple with an Omron E5CK PID controller. The temperature in the catalyst bed was measured with an internal thermocouple to confirm the absence of radial temperature gradients. A backpressure of 1.8 barg is used for all experiments. Manometers at the entrance and outlet of the reactor allowed verifying the absence of a significant pressure drop over the reactor. A three-way valve after the backpressure valve allowed to periodically draw samples from the reactor effluent.

Sample analysis. The reaction samples were analyzed using a reversed-phase high-performance liquid chromatograph (RP-HPLC) from Agilent (1100 series) using the same procedure as reported before[33]. The HPLC Eclipse XDB-C18 column was operated at 30 °C using a gradient method with water (0.1% trifluoroacetic acid, Acros) and 30 v% to 62 v% acetonitrile (HPLC grade, Acros) as solvents. This method separates all the components in a period of 14 min. The components were identified using a UV-detector with a variable wavelength that has been programmed for an optimal absorption for each component. Quantification of the different components in the reaction mixture was performed by relating the surface areas of the component peaks to the amount of internal standard added to the reactor.

Determination of catalytic activity and 4-nitrobenzaldehyde molar balance. The total product yield is defined by the sum of the aldol and enone product concentration divided by the initial concentration of 4-nitrobenzaldehyde. The specific catalytic activity ($mol_{product}\ g_{catalyst}^{-1}\ s^{-1}$) was determined by considering the slope of the stable linear part in the graph of the total product yield as a function of reaction time in batch, multiplied by the amount of catalyst. The site time yield ($mol_{product}\ mol_{sites}^{-1}\ s^{-1}$) was defined by dividing the specific catalytic activity by active site concentration ($mol_{sites}\ g_{catalyst}^{-1}$), as determined from elemental analysis. The 4-nitrobenzaldehyde molar balance (Δ) was defined for each sample by relating the sum of the concentration of 4-nitrobenzaldehyde, aldol product, and enone product to the initially added concentration of 4-nitrobenzaldehyde (eq. 2).

$$\Delta(t) = \frac{C_{4-NB,t} + C_{aldol,t} + C_{enone,t}}{C_{4-NB,0}} \quad \text{(eq. 2)}$$

Results and Discussion

The catalytic activity of chitosan in its crude form, as hydrogel and as aerogel is evaluated in a batch reactor for the aldol reaction of acetone with 4-nitrobenzaldehyde using a mixture of water and acetone as solvent. To assess the stability of the catalyst, a recycle experiment is performed. Additionally, the catalyst stability is also evaluated by measuring the total product yield as a function of time on stream in a continuous-flow reactor. Finally, the activity of the primary amine sites as a function of the degree of deacetylation (DDA) is investigated, and guidelines are provided for further catalyst improvement.

Kinetic investigation of chitosan in a batch reactor

In all experiments the aldol product is found as major primary reaction product, with a selectivity ranging from 100% at the beginning of the reaction to 98% after 4 hours of reaction. Correspondingly, the selectivity towards the dehydrated enone product ranges from 0% selectivity at the beginning of the reaction up to 2%. No reaction products of the acetone self-aldolization were detected.

Crude Chitosan. The measured total product yield obtained with crude low-molecular weight chitosan as catalyst in the aldol reaction of acetone with 4-nitrobenzaldehyde, as a function of time, is displayed in Figure 3. Two different regions, indicated by grey and black symbols, can be distinguished. Initially, the slope of the curve decreases up to 2 hours of reaction, after which it appears to remains constant. This trend is not expected for a simple reaction in a batch reactor, which should exhibit a linear trend initially followed by a gradually decreasing slope at higher conversions. This deviating trend indicates that specific phenomena occur initially, leading to a decrease in the reaction rate, until a constant residual reaction rate remains, e.g., because the phenomenon has been equilibrated.

The 4-nitrobenzaldehyde molar balance for the liquid phase in this experiment, shown in the Supplementary Information in Figure 2S, decreased from 100% at the start of the reaction asymptotically to 78%. This means that 22% of the 4-nitrobenzaldehyde fed in the reaction is converted to other products than the reaction products. Because no additional products have been detected in the liquid phase during HPLC analysis, it is likely that part of the 4-nitrobenzaldehyde remains adsorbed on the active sites. Previously, it has been suggested that stable imines derived from 4-nitrobenzaldehyde can form on primary amines and inhibit the aldol reaction[36].

In the considered reaction mechanism, displayed in Figure 2, two different imines involving 4-nitrobenzaldehyde occur, i.e. species **5** and species **8**. The latter is more stable towards hydration due to conjugation with the aromatic ring and is, hence, expected to act as an inhibiting species.

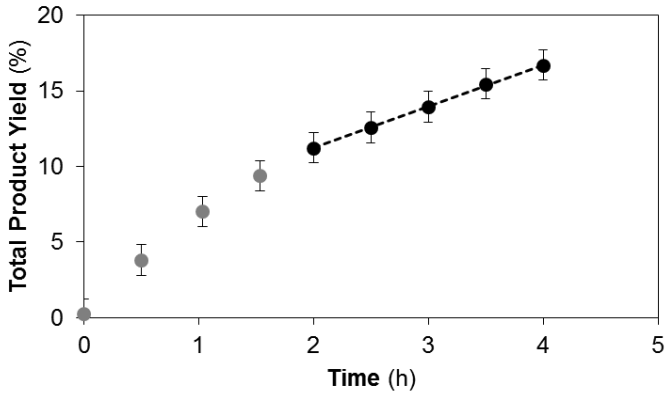

Figure 3: Total product yield versus reaction time for crude low-molecular weight chitosan as catalyst in the aldol reaction of acetone with 4-nitrobenzaldehyde. (T = 55 °C, $m_{acetone}$ = 45 g, m_{4NB} = 0.45 g, m_{water} = 55 g, $m_{chitosan}$ = 0.26 g)

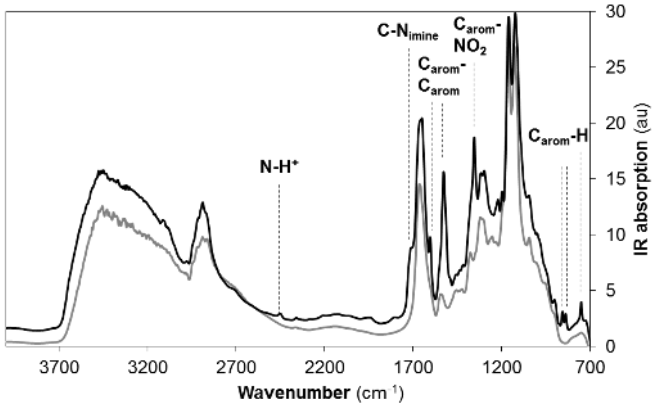

Figure 4: IR spectrum of fresh (grey) and spent (black) chitosan for the aldol reaction of acetone with 4-nitrobenzaldehyde employing water as solvent. (T = 55 °C, $m_{acetone}$ = 45 g, m_{4NB} = 0.45 g, m_{water} = 55 g, $m_{chitosan}$ = 0.26 g)

Reactions that consume this imine intermediate (**8**), such as Mannich-type addition reactions, would require activating acetone towards its enol or enolate intermediate with a strong homogeneous acid or base and, hence, are expected to be of minor importance at the investigated reaction conditions[34]. Moreover, the primary product of this Mannich-type addition reaction would be the enone product, which is in this work observed as a secondary product resulting from the aldol product dehydration, as displayed in Figure 3S in the Supplementary Information. The formation of imine species **8** thus allows rationalizing the primary amine site inhibition.

It is indeed generally known that the primary amines on chitosan can form imines, with the release of water, when reacting with aldehydes or ketones[11, 51, 52]. It is, however, assumed that hydrolysis of the imine is fast in aqueous conditions, and thereby shifts the equilibrium away from the imine[36, 53]. Figure 4 shows an FTIR spectrum of fresh and spent crude chitosan used in the aldol reaction from which it does appear that, under the employed reaction conditions, a stable imine of a 4-nitrobenzaldehyde containing species can form on the primary amines. Three small peaks appear in the spectrum of the spent catalyst in the region of 700 cm^{-1} to 900 cm^{-1}, indicative of the C-H vibrations in aromatic molecules. The large peak at 1529 cm^{-1} and the shoulder at 1620 cm^{-1} further indicates aromatic species, while the peak at 1356 cm^{-1} can be attributed to a NO_2 group attached to the aromatic ring. A small shoulder at 1690 cm^{-1}, next to the known amide stretch peak, indicates the C-N stretch of an imine. The small peak at 2460 cm^{-1} is due to the $N\text{-}H^+$ stretch of protonated amine or imine species. While peaks that signify the presence of an imine are close to those that indicate the presence of aldehyde groups, it is unlikely that the aldehyde form of 4-nitrobenzaldehyde as such is present on the material because the spent chitosan was washed twice in deionized water before analysis.

Under the employed reaction conditions in the batch reactor, the decrease of the 4-nitrobenzaldehyde molar balance equilibrated at 78%, which amounts to 0.60 mmol of 4-nitrobenzaldehyde-containing species being adsorbed as imines. This amounts to 52% of the primary amine sites on chitosan that have been inhibited by an imine of 4-nitrobenzaldehyde.

A 24 hour 4-nitrobenzaldehyde adsorption equilibrium test was also performed with crude chitosan, under exactly the same conditions as the catalytic experiments, except that acetone was replaced by DMSO. It was calculated from the decrease in the liquid phase 4-nitrobenzaldehyde concentration that adsorption had occurred on almost half of the primary amine sites. The FTIR spectrum of this chitosan catalyst is displayed in Figure 5S in the Supplementary Information and exhibits the same characteristic peaks as the ones observed in Figure 4. This further points into the direction that the species detected on the spent catalyst is indeed species **8** in Figure 2 which is formed by interaction of 4-nitrobenzaldehyde with the primary amine.

The reaction rate measured for crude chitosan in the linear regime observed in Figure 3, where it is assumed that the inhibition phenomena have been equilibrated, amounts to 8.87 ± 0.21 10^{-5} $mol_{products}$ $kg_{chitosan}^{-1}$ s^{-1}, as displayed in Table 1. Elemental analysis indicated a degree-of-deacetylation of 70.5 ± 3.5 %, which results in an average site time yield of 2.18 ± 0.05 10^{-5} $mol_{product}$ mol_{amine}^{-1} s^{-1} considering all primary amine sites, i.e., including the inhibited sites.

Chitosan Hydrogels and Aerogels. Chitosan hydrogels of ± 2 mm diameter are synthesized according to known literature procedures[10], and have also been evaluated in the aldol reaction of acetone with 4-nitrobenzaldehyde. For these catalytic performance tests, the chitosan mass was determined by drying a part of the hydrogel beads, and has been kept constant as compared to the other experiments. The total product yield as a function of reaction time is given in Figure 5 for a first and a consecutive run. The first catalytic run exhibited the same behavior as crude chitosan, i.e., a decrease in slope until 2 hours of reaction after which the slope remained constant until the end of the reaction. The reaction rate measured in this linear regime amounts to 8.96 ± 0.74 10^{-5} $mol_{product}$ $kg_{chitosan}^{-1}$ s^{-1} and the corresponding site time yield to 2.21 ± 0.18 10^{-5} $mol_{product}$ mol_{site}^{-1} s^{-1}, see Table 1. The catalytic activity of chitosan hydrogels, calculated based on the equivalent of chitosan in the hydrogel, is thus found to be within the error margin of crude chitosan. This shows that there is no structural difference between hydrated crude chitosan and hydrogels as catalysts in the aldol reaction. The second run exhibited a linear evolution over the entire duration of the

experiment, indicating that the inhibitory imine formation on the surface is equilibrated from the start of the experiment. Even though much lower yields were obtained in a second run, the slope of the yield versus time curve is approximately identical to the slope at higher conversions observed during the first run. Comparing these slopes, a reusability ratio of 82% is found. However, it should be noted that the mechanical stirring in the Parr® reactor caused the hydrogel beads to break. Hence, a smaller scale experiment in glassware was also conducted, under less severe stirring, for which a reaction rate of 2.16 ± 0.10 10^{-5} $mol_{product}$ mol_{amine}^{-1} s^{-1} was found and a 95 ± 10 % reusability ratio. The total product yield curve versus time for this experiment is displayed in Figure 4S in the Supplementary Information.

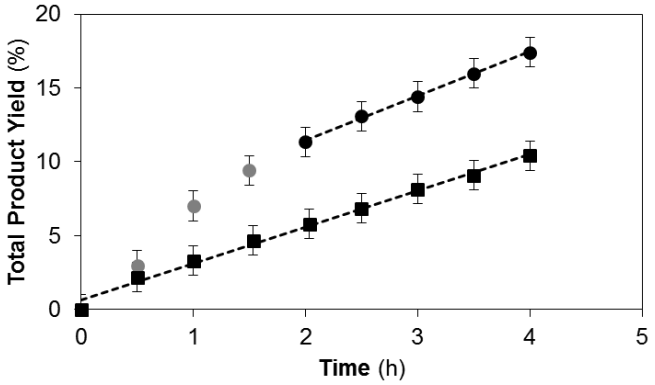

Figure 5: Total product yield versus reaction time for hydrogels of low-molecular weight chitosan as catalyst in the aldol reaction of acetone with 4-nitrobenzaldehyde. First run (●) second run (■). (T = 55 °C, $m_{acetone}$ = 45 g, m_{4NB} = 0.45 g, m_{water} = 55 g, $m_{chitosan}$ = 0.26 g)

Chitosan aerogels were synthesized by lyophilization of the hydrogel beads. Again, the same behavior in the total product yield versus reaction time is observed, i.e., a gradually decreasing slope until 2 hours of reaction, after which a more stable regime is reached. The slope of the linear part of the yield versus time graph for the chitosan aerogels results in an activity of 8.51 ± 0.43 10^{-5} $mol_{product}$ $kg_{chitosan}^{-1}$ s^{-1} and a site time yield of 2.09 ± 0.11 10^{-5} $mol_{product}$ mol_{amine}^{-1} s^{-1}. Also, in this case the reaction rate appears to be the same, within the experimental error margin, as compared to crude chitosan and chitosan hydrogels. All values are summarized Table 1. The second run in the Parr reactor using chitosan aerogels resulted in a reusability ratio of 90 ± 10 %. The above observations indicate that the catalytic activity in the linear regime of the yield versus time curve of the first run can be reproduced in the second one and, hence, that hydrogel and aerogel catalysts are reusable without quantifiable activity losses.

Stability of crude chitosan under continuous-flow

It was described previously how the chitosan hydrogel and aerogel catalyst were recycled for a second run in a batch reactor and the original activity could be reproduced. To assess the long-term stability of crude chitosan under reaction conditions, without filtering and recycling the catalyst after each run, a continuous-flow reactor loaded with a packed bed has been employed under exactly the same operating conditions as in the batch reactor.

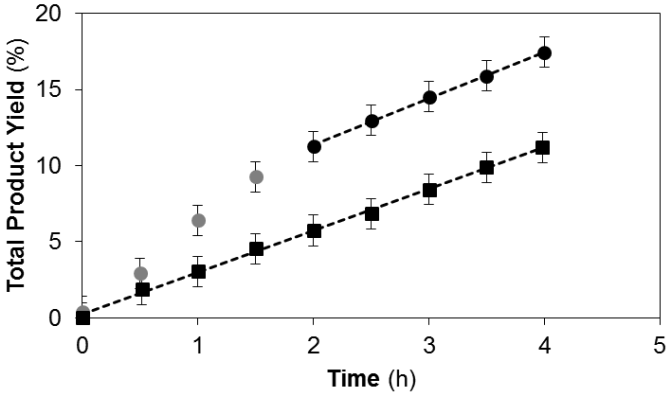

Figure 6: Total product yield versus reaction time for aerogels of low-molecular weight chitosan as catalyst in the aldol reaction of acetone with 4-nitrobenzaldehyde. First run (●) second run (■). (T = 55 °C, $m_{acetone}$ = 45 g, m_{4NB} = 0.45 g, m_{water} = 55 g, $m_{chitosan}$ = 0.26 g)

The total product yield for the aldol reaction in the continuous-flow reactor is given as a function of the time-on-stream in Figure 7. Sampling was only started after 1 hour on stream because, from the reactor hydrodynamics point of view, no steady-state operation was obtained in this first hour of reaction. From 1 hour on-stream up to 4.5 hours on-stream, the total product yield decreased gradually. This is attributed to the formation of stable imines derived from 4-nitrobenzaldehyde, in line with the observations made in the batch reactor. From 4.5 hours on-stream onwards, the inhibitory phenomena have stabilized and a stable total product yield is obtained. The 4-nitrobenzaldehyde molar balance also equilibrated after 4.5 hours on stream around 100%. This indicates that the adsorption of 4-nitrobenzaldehyde as imine species on the surface has reached an equilibrium. These results indicate that, even though the imine formation is inhibiting active sites on chitosan and leading to a lower observed product yield, a stable operating regime can be reached in the continuous-flow aldol reaction with water as co-solvent. This is in contrast with the current state-of-the-art aminated mesoporous silica catalysts that were found to continuously deactivate due to silica hydrolysis and leaching caused by water[33, 38].

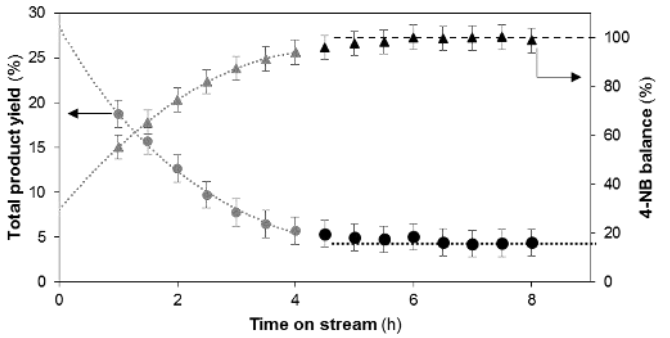

Figure 7: Total product yield (●, left axis) and 4-nitrobenzaldehyde molar balance (▲, right axis) as a function of time-on-stream in the continuous-flow reactor using crude chitosan as catalyst. ($W/F^0_{4\text{-}NB}$ = 1510 kg_{cat} s mol^{-1}_{4NB}, 44.7 wt% acetone, 54.6 wt% water, 0.45 wt% 4-nitrobenzaldehyde, 0.20 wt% methyl-4-nitrobenzoate, T = 55 °C).

Table 1: Summary of the reaction rate on a mass basis, site time yield, and reusability in a second 4 hour run for the different chitosan catalysts. (*reusability was evaluated in smaller glass batch-type reactor) (T = 55 °C, $m_{acetone}$ = 45 g, m_{4NB} = 0.45 g, m_{water} = 55 g, $m_{chitosan}$ = 0.26 g)

Chitosan Catalyst	Reaction rate 10^{-5} ($mol_{product}$ $kg_{chitosan}^{-1}$ s^{-1})	Site time yield 10^{-5} ($mol_{product}$ mol_{amine}^{-1} s^{-1})	Reusability (%)
Crude	8.87 ± 0.21	2.18 ± 0.05	-
Hydrogel	8.96 ± 0.74	2.21 ± 0.18	*95 ± 10
Aerogel	8.51 ± 0.43	2.09 ± 0.11	90 ± 10

Amine activity as a function of the degree-of-deacetylation

Chitin was found to possess a degree-of-deacetylation (DDA) of 2.6 ± 3.5% and was also evaluated for the aldol reaction. The primary amines in chitin yielded a site time yield of 15.40 ± 0.07 10^{-5} $mol_{product}$ mol_{amine}^{-1} s^{-1}, which exceeds that observed by the chitosan catalysts with a DDA of 70.4 ± 3.5 % by almost a factor 8. Additionally, in-house synthesized chitosan catalysts, in powder form, with a DDA varying between 13.1 ± 3.5 % and 76.8 ± 3.5 % were also evaluated. Their site time yield (STY) was determined in the region between 2 hours and 4 hours of reaction and is reported in Figure 8 as a function of their DDA.

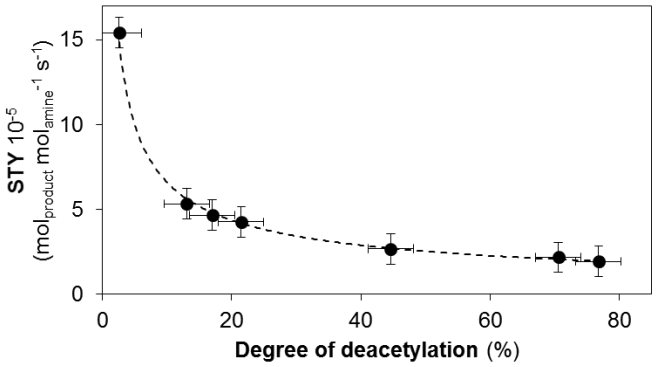

Figure 8: Site time yield for primary amines in deacetylated chitin from 2.6% to 76.8% deacetylation. Line is a guide for the eye. (T = 55 °C, $m_{acetone}$ = 45 g, m_{4NB} = 0.45 g, m_{water} = 55 g, $m_{chitosan}$ = 0.26 g, Parr reactor)

As the DDA increased, the primary amine concentration increased, and the site time yield decreased, as displayed in Figure 8. Table 2 indicates that the increase in active site concentration appears to compensate for the loss in site time yield and therefore results in an increasing catalytic activity on a mass basis. This site time yield decrease with increasing DDA can be attributed to a decrease in the primary amine basicity from a pKa of 10.44, when chitosan is almost fully acetylated, to a pKa of 5.44 upon full deacetylation[54]. The increased hydrophobicity upon acetylation has been deemed responsible for differences in electrostatic properties, leading, in turn, to the change in amine pKa with DDA[54]. The amine sites in chitosan with a low DDA, hence, appear to exhibit a basicity close to that of a simple primary amine with a short alkyl chain, such as those typically grafted on mesoporous silica[35].

Primary amine grafted mesoporous silica catalysts, evaluated using hexane as solvent, exhibited a site time yield of 78.0 10^{-5} s^{-1} in the presence of an excess of cooperative silanol groups and 20.0 10^{-5} s^{-1} without such silanol groups[35]. While comparison should be performed carefully because of differences in solvent and morphology can lead to a different sorption behavior[55], the value of the unpromoted primary aminated silica catalysts appears to be in the same order of magnitude as the value reported in Table 2 for chitosan with the lowest DDA.

These results indicate that further improvement of the catalytic activity of chitosan is possible by tuning the electrostatic properties of the material, such that the pKa of the amine sites is increased. Combined with the high loadings that are possible on these materials, and their stability in an aqueous environment, promising new heterogeneous catalysts can be developed for the aldol reaction.

Conclusions

The reaction rate of the primary amine sites in chitosan with a degree-of-deacetylation (DDA) of 70.4% has been quantified for the first time in this work for the aldol reaction of acetone with 4-nitrobenzaldehyde. During the first 2 hours in the batch reactor, a stable imine derived from 4-nitrobenzaldehyde was formed on the primary amine sites, which blocked access to the active site and decreased the observed catalytic activity. When the imine formation has equilibrated, a stable catalytic activity of 2.18 ± 0.05 10^{-5} $mol_{product}$ mol_{amine}^{-1} s^{-1} was obtained. Changing the morphology of the catalyst to a hydrogel via reprecipitation, or an aerogel via lyophilization, did not affect the intrinsic catalytic activity of the primary amine in the catalyst. Chitosan hydrogels and aerogels were recycled in the batch reactor and allowed reproducing the original activity when the inhibitory phenomena were equilibrated. The long term stability of crude chitosan was then evaluated for the first time in a continuous-flow reactor, under the same reaction conditions as the batch reactor. The activity showed first an exponential decrease due to imine formation, followed by a stable regime. This remarkable stability is a desirable property for a heterogeneous catalyst in the aqueous aldol reaction. The site time yield of the primary amines in commercial chitin with a DDA of 2.6% amounted to 15.40 ± 1.39 10^{-5} $mol_{product}$ mol_{amine}^{-1} s^{-1}, which is in the same order of magnitude as the literature reported unpromoted primary amine functionalized silica catalysts evaluated in hexane. Increasing the degree of deacetylation, however, causes a decrease in the site time yield due to a corresponding decrease in amine pKa. Further catalyst improvement can thus be situated in the development of amine sites with a high pKa, which is independent from the amine loading on the polymer backbone.

Table 2: Summary of reaction rate and site time yield for chitosan with a different degree-of-deacetylation (DDA). (T = 55 °C, $m_{acetone}$ = 45 g, m_{4NB} = 0.45 g, m_{water} = 55 g, $m_{chitosan}$ = 0.26 g, Parr reactor)

DDA (%) ± 3.5 %	Primary amines (mmol/g)	Reaction rate 10^{-5} ($mol_{product}$ $kg_{chitosan}^{-1}$ s^{-1})	Site time yield 10^{-5} ($mol_{product}$ mol_{amine}^{-1} s^{-1})
2.6	0.13	1.97 ± 0.18	15.40 ± 1.39
13.1	0.66	3.48 ± 0.31	5.31 ± 0.48
17.0	0.87	4.03 ± 0.36	4.64 ± 0.42
21.5	1.11	4.55 ± 0.41	4.25 ± 0.38
44.6	2.42	6.53 ± 0.59	2.66 ± 0.24
76.7	4.49	8.83 ± 0.79	1.92 ± 0.17

Conflicts of interest

There are no conflicts to declare

Acknowledgements

The authors acknowledge financial support from the Research Foundation - Flanders (FWO) through Grant Number 3G006813 and the European Research Council under the European Union's Seventh Framework Programme (FP7/2007-2013) / ERC grant agreement n°615456. J.L. is a postdoctoral fellow of the Research Foundation – Flanders (FWO) (12Z2218N). The authors would like to thank Eli Moens for the help with the catalytic experiments. JWT acknowledges the ERC for the PoC Grant SERENiTi (GA n°825783).

Notes and references

1. A. El Kadib, *ChemSusChem*, 2015, **8**, 217-244.
2. T. G. Asere, S. Mincke, J. De Clercq, K. Verbeken, D. A. Tessema, F. Fufa, C. V. Stevens and G. Du Laing, *International journal of environmental research and public health*, 2017, **14**, 895.
3. S. Mincke, T. G. Asere, I. Verheye, K. Folens, F. V. Bussche, L. Lapeire, K. Verbeken, P. Van Der Voort, D. A. Tessema and F. Fufa, *Green Chemistry*, 2019.
4. E. Schoolaert, I. Steyaert, G. Vancoillie, J. Geltmeyer, K. Lava, R. Hoogenboom and K. De Clerck, *Journal of Materials Chemistry B*, 2016, **4**, 4507-4516.
5. A. Verlee, S. Mincke and C. V. Stevens, *Carbohydrate polymers*, 2017, **164**, 268-283.
6. E. I. Rabea, M. E.-T. Badawy, C. V. Stevens, G. Smagghe and W. Steurbaut, *Biomacromolecules*, 2003, **4**, 1457-1465.
7. K. R. Reddy, K. Rajgopal, C. U. Maheswari and M. L. Kantam, *New journal of chemistry*, 2006, **30**, 1549-1552.
8. C. Gioia, A. Ricci, L. Bernardi, K. Bourahla, N. Tanchoux, M. Robitzer and F. Quignard, *European Journal of Organic Chemistry*, 2013, **2013**, 588-594.
9. A. Ricci, L. Bernardi, C. Gioia, S. Vierucci, M. Robitzer and F. Quignard, *Chemical communications*, 2010, **46**, 6288-6290.
10. D. Kühbeck, G. Saidulu, K. R. Reddy and D. D. Díaz, *Green chemistry*, 2012, **14**, 378-392.
11. H. Kayser, C. R. Müller, C. A. García-González, I. Smirnova, W. Leitner and P. D. de María, *Applied Catalysis A: General*, 2012, **445**, 180-186.
12. O. Mahé, J. F. Brière and I. Dez, *European Journal of Organic Chemistry*, 2015, **2015**, 2559-2578.
13. H. Zhang, W. Zhao, J. Zou, Y. Liu, R. Li and Y. Cui, *Chirality: The Pharmacological, Biological, and Chemical Consequences of Molecular Asymmetry*, 2009, **21**, 492-496.
14. T. Jose, N. Sudheesh and R. S. Shukla, *Journal of Molecular Catalysis A: Chemical*, 2010, **333**, 158-166.
15. H. Suwito, Jumina, Mustofa, A. N. Kristanti and N. N. T. Puspaningsih, *Journal of Chemical and Pharmaceutical Research*, 2014, **6**, 1076-1088.
16. G. Kelly, F. King and M. Kett, *Green Chemistry*, 2002, **4**, 392-399.
17. S. Cheng, X. Wang and S.-Y. Chen, *Topics in Catalysis*, 2009, **52**, 681-687.
18. J. N. Chheda and J. A. Dumesic, *Catalysis Today*, 2007, **123**, 59-70.
19. J. Xie, L. Zhang, X. Zhang, P. Han, J. Xie, L. Pan, D.-R. Zou, S.-H. Liu and J.-J. Zou, *Sustainable Energy & Fuels*, 2018, **2**, 1863-1869.
20. R. Xing, A. V. Subrahmanyam, H. Olcay, W. Qi, G. P. van Walsum, H. Pendse and G. W. Huber, *Green Chemistry*, 2010, **12**, 1933-1946.
21. Q. Deng, J. Xu, P. Han, L. Pan, L. Wang, X. Zhang and J.-J. Zou, *Fuel Processing Technology*, 2016, **148**, 361-366.
22. C. Lucarelli and A. Vaccari, *Green Chemistry*, 2011, **13**, 1941-1949.
23. P. M. Price, J. H. Clark and D. J. Macquarrie, *Journal of the Chemical Society, Dalton Transactions*, 2000, 101-110.
24. E. Dumitriu, V. Hulea, I. Fechete, A. Auroux, J.-F. Lacaze and C. Guimon, *Microporous and Mesoporous Materials*, 2001, **43**, 341-359.
25. A. Ungureanu, S. Royer, T. V. Hoang, D. Trong On, E. Dumitriu and S. Kaliaguine, *Microporous and Mesoporous Materials*, 2005, **84**, 283-296.
26. L. Hora, V. Kelbichová, O. Kikhtyanin, O. Bortnovskiy and D. Kubička, *Catalysis Today*, 2014, **223**, 138-147.
27. L. Hora, O. Kikhtyanin, L. Čapek, O. Bortnovskiy and D. Kubička, *Catalysis Today*, 2015, **241**, 221-230.
28. N. A. Brunelli and C. W. Jones, *Journal of Catalysis*, 2013, **308**, 60-72.
29. S. Shylesh, D. Hanna, J. Gomes, S. Krishna, C. G. Canlas, M. Head-Gordon and A. T. Bell, *ChemCatChem*, 2014, **6**, 1283-1290.
30. Y. Kubota, H. Yamaguchi, T. Yamada, S. Inagaki, Y. Sugi and T. Tatsumi, *Topics in Catalysis*, 2010, **53**, 492-499.
31. N. A. Brunelli, K. Venkatasubbaiah and C. W. Jones, *Chemistry of Materials*, 2012, **24**, 2433-2442.
32. J. Lauwaert, E. De Canck, D. Esquivel, J. W. Thybaut, P. Van Der Voort and G. B. Marin, *ChemCatChem*, 2014, **6**, 255-264.
33. A. De Vylder, J. Lauwaert, D. Esquivel, D. Poelman, J. De Clercq, P. Van Der Voort and J. W. Thybaut, *Journal of Catalysis*, 2018, **361**, 51-61.
34. K. Kandel, S. M. Althaus, C. Peeraphatdit, T. Kobayashi, B. G. Trewyn, M. Pruski and I. I. Slowing, *ACS Catalysis*, 2013, **3**, 265-271.
35. J. Lauwaert, E. De Canck, D. Esquivel, P. Van Der Voort, J. W. Thybaut and G. B. Marin, *Catalysis Today*, 2015, **246**, 35-45.
36. K. Kandel, S. M. Althaus, C. Peeraphatdit, T. Kobayashi, B. G. Trewyn, M. Pruski and I. I. Slowing, *Journal of Catalysis*, 2012, **291**, 63-68.
37. A. De Vylder, J. Lauwaert, M. K. Sabbe, M.-F. Reyniers, J. De Clercq, P. Van Der Voort and J. W. Thybaut, *Catalysis Today*, 2019.
38. M. Etienne and A. Walcarius, *Talanta*, 2003, **59**, 1173-1188.
39. S. Bahmanyar and K. Houk, *Journal of the American Chemical Society*, 2001, **123**, 11273-11283.
40. K. Okuyama, K. Noguchi, T. Miyazawa, T. Yui and K. Ogawa, *Macromolecules*, 1997, **30**, 5849-5855.
41. M. Rinaudo, *Progress in polymer science*, 2006, **31**, 603-632.
42. E. F. Franca, R. D. Lins, L. C. Freitas and T. Straatsma, *Journal of Chemical Theory and Computation*, 2008, **4**, 2141-2149.
43. C. Hammond, *Green Chemistry*, 2017, **19**, 2711-2728.
44. K. Ogawa, T. Yui and M. Miya, *Bioscience, biotechnology, and biochemistry*, 1992, **56**, 858-862.
45. M. H. Mohammed, P. A. Williams and O. Tverezovskaya, *Food Hydrocolloids*, 2013, **31**, 166-171.
46. M. R. Kasaai, J. Arul and G. Charlet, *Journal of Polymer Science Part B: Polymer Physics*, 2000, **38**, 2591-2598.
47. K. Gupta and F. H. Jabrail, *Carbohydrate Polymers*, 2006, **66**, 43-54.
48. Z. Dos Santos, A. Caroni, M. Pereira, D. Da Silva and J. Fonseca, *Carbohydrate Research*, 2009, **344**, 2591-2595.
49. N. C. Ellebracht and C. W. Jones, *Cellulose*, 2018, **25**, 6495-6512.
50. X. Zhang and K. N. Houk, *The Journal of Organic Chemistry*, 2005, **70**, 9712-9716.
51. L. Marin, B. Simionescu and M. Barboiu, *Chemical Communications*, 2012, **48**, 8778-8780.
52. J. E. dos Santos, E. R. Dockal and É. T. G. Cavalheiro, *Carbohydrate Polymers*, 2005, **60**, 277-282.

53. K. d. Yao, T. Peng, M. x. Xu, C. Yuan, M. F. Goosen, Q. q. Zhang and L. Ren, *Polymer international*, 1994, **34**, 213-219.
54. P. Sorlier, A. Denuzière, C. Viton and A. Domard, *Biomacromolecules*, 2001, **2**, 765-772.
55. J. Lauwaert, J. Ouwehand, J. De Clercq, P. Cool, P. Van Der Voort and J. W. Thybaut, *Catalysis Communications*, 2017, **88**, 85-89.